ORIGINAL PAPER

Distiller's Grain-Derived Biochar as Novel Soil Amendment Benefits Growth and Decreases Cd Uptake of Wheat by Modifying Cd Fractions and Rhizospheric Microbiota

Chengyu Wang[1,2] · Jieming Li[1] · Lujun Chen[3] · Xin Huang[4]

Abstract

This study aimed to explore natural aging effect of distiller's grain-derived biochar (DGB) at various amendment rates (2%, 4%, w/w) on wheat (*Triticum aestivum* L.) growth, development and Cd uptake in soil, and provide novel insights in effect mechanisms from views of soil Cd fractions and rhizospheric microbiota. Results showed that DGB amendment promoted wheat growth. Rising DGB rate progressively increased soil pH, soil organic matter (SOM), total carbon (TC), total nitrogen (TN), NH_4-N, available K, and residual Cd content to more greatly promote chlorophyll content and decrease Cd uptake of wheat. With 6-month aging, soil TN, available K and residual Cd content continuously increased to decline Cd bioavailability, which further restricted Cd uptake by wheat roots, stems, and leaves, and did not obviously change Cd uptake by wheat grains. Contrarily, soil NO_3-N content progressively decreased with rising DGB rate and aging, partly due to progressively decreased nitrifier abundances of Nitrosomonadaceae and Nitrospiraceae with rising DGB rate and aging, according to rhizospheric bacterial composition. Statistical analysis verified that DGB rate and aging were synergistic factors to jointly involve soil nutrient increase and Cd fractions re-distribution. Rising DGB rate and aging jointly increased the abundances of Actinobacteria, Cyanobacteria, and Fibrobacteria phyla, and *Lysobacter*, *Massilia*, *Pseudarthrobacter*, and *Iamia* genera that positively correlated to soil residual Cd, TN, SOM, TC, and available K content, suggesting that such bacterial groups also drove soil fertility improvement and Cd bioavailability decrease. Consequently, amending 4% DGB with aging was proposed as appropriate for improving soil fertility and blocking Cd-induced health risk.

Keywords Cadmium · Distiller's grain-derived biochar · Natural aging · Rhizospheric bacterial composition · Soil nutrient · Wheat

1 Introduction

Soil cadmium (Cd) pollution is highly severe and major concern in China (Hamid et al. 2020; Yuan et al. 2021a). Cd bioavailability relies on Cd fractions distribution, including acid-soluble, reducible, oxidizable, and residual fractions with decreasing bioavailability in sequence, which affect crop growth and Cd uptake (Chen et al. 2019). Wheat is cereal crop for global consumption but susceptible to Cd uptake. Cd can transfer to aboveground part and accumulate in wheat grains to endanger human health (Zhou et al. 2020; Wang et al. 2021). Seeking eco-benign option for declining Cd bioavailability to alleviate Cd uptake and promote wheat growth is desirable.

Biochar, a carbonaceous material derived from biomass, always act as soil amendments and pollution-remediating agents (Beesley et al. 2011; Shaheen et al. 2018; Yuan et al. 2021b; Zhang et al. 2021). Biochar can decrease soil heavy metal (HM) bioavailability via oxidation/reduction and complexes formation and/or via sorption by porous structure and functional groups (Zhang et al. 2013; Rehman et al. 2016; Zhao and Li 2022). Distiller's grains (DGs) are main

✉ Jieming Li
lijieming@cau.edu.cn

[1] College of Resources and Environmental Sciences, China Agricultural University, Beijing 100193, China

[2] Organic Recycling Institute (Suzhou), China Agricultural University, Suzhou 215128, Jiangsu, China

[3] School of Environment, Tsinghua University, Beijing 100084, China

[4] College of Biomass Science and Engineering, Sichuan University, Chengdu 610065, China

by-product of white-spirit industry with sorghum and rice husks as raw materials and often used as animal feed or randomly discarded. A huge amount of DGs are generated annually by Chinese white-spirit industry, and improper DGs disposal undoubtedly causes pollution and resource-wasting (Lian et al. 2019; Liu et al. 2022). Recycling DGs is vital to lessen DG-caused environmental burdens. Because DGs hold massive digestible fiber, polysaccharide, and protein due to starch removal during fermentation, it is feasible to convert DGs into biochar for Cd-immobilization (Cheng et al. 2021), which promotes DGs' added value and sustainable development of brewing industry. Using DG-derived biochar (DGB) for aqueous HM-removal attracted recent interests (Zhang et al. 2016; Lian et al. 2019; Zhao and Li 2022), but few study applied DGB to immobilize soil Cd and mitigate agro-food risk, which merits urgent research.

Once amended in soils, biochar interacts with soil matrix and biochemical processes occur on biochar-soil interface (so-called natural aging) to alter biochar properties and thus modify biochar's effects on soil Cd bioavailability (Zhang et al. 2016; Tan et al. 2020). Using biochars formed at 550–650 °C, Nie et al. (2021) showed stronger Cd sorption by aged than fresh biochar-amended soils (0.5–2%, w/w) regardless of biochar's precursors, whereas Bandara et al. (2021) found that Cd bioavailability declined in poultry litter biochar-amended soils but increased in wood biochar-amended soils (3%, w/w) after natural aging. These indicated that natural aging effect of biochar on soil Cd bioavailability could differ with biochar's precursors and thus requires further study on case-by-case basis to avoid adverse effect. Notably, many artificial aging methods (e.g., dry–wet/freeze–thaw cycle, chemical oxidation) cannot simulate and actually reflect natural aging effect of biochar, because natural aging induces complex biochemical processes that cannot be realized during artificial aging (Qian and Chen 2014; Tan et al. 2020; Meng et al. 2022). To date, research on natural aging effects of biochar on soil Cd bioavailability and wheat growth in Cd-laden soil, as well as effect mechanisms, were still quite rare and insufficient, especially how natural aging influenced DGB's properties and effects on wheat growth and Cd uptake by altering soil Cd fraction distribution was unclear. Exploring this concern would help to optimize DGB-amending scheme to mitigate Cd-induced agro-food risk.

Bacterial community as soil quality indicator can improve soils to directly affect soil HMs' bioavailability, during which key bacterial abundance changes (Huang et al. 2017; Wang et al. 2020a). Rhizospheric bacterial composition may change in response to changing soil properties caused by DGB amendment with aging and in turn alter wheat growth and Cd uptake, but how natural aging of biochar in soil affected bacterial community's role in regulating soil Cd bioavailability, wheat growth, and Cd uptake are always ignored. Exploring natural aging effect of DGB on rhizospheric microbiota in Cd-laden soil can reveal effect mechanisms from microbial insight.

To fill above gaps, this study explored the effect of different DGB-amending schemes on Cd fractions distribution, wheat growth, Cd uptake, and rhizospheric bacterial composition in Cd-laden soil, where DGB was amended at various rates without aging (fresh) or with 6-month aging in soil. All DGB-amended soils were characterized. At different DGB-amending schemes, wheat growth and Cd uptake were measured, and soil Cd fractions reflecting Cd bioavailability and rhizospheric bacterial composition were determined to interpret regulatory effect mechanisms. Results shed novel insights in effect mechanisms of different DGB-amending schemes on wheat growth and Cd uptake and guided to feasibly amending DGB to block soil Cd-pollution and increase soil fertility and agro-food safety.

2 Materials and Methods

2.1 Soil Collection and DGB Preparation

Soil was collected from 0 to 15 cm layer at Shangzhuang Experimental Station (40°08′ 21″N, 116°10′ 52″E) of China Agricultural University in Beijing, China. Air-dried soil was milled to pass through 2 mm size-sieve and pre-incubated at 25 °C for a week to stabilize bioactivity. The soil was HM-free soil (Table S1), according to environment quality risk control standard for soil contamination of agricultural land (GB15618-2018). DGs obtained from Luzhou Laojiao Co. Ltd. were by-products of liquor, with sorghum and rice-husk as main and auxiliary material, respectively, and mainly contained cellulose, hemicellulose, sugar, proteins, and nutrient components. Air-dried DGs were pyrolyzed into DGB at 600 °C for 2 h with heating rate of 5–10 °C/min under oxygen-limited conditions in a muffle furnace, and the DGB was milled to pass through 2 mm-size sieve before experiment. DGB characterization procedure was described in Supplementary Information.

2.2 Pot experiment Design

Cd was spiked at 20 mg kg^{-1} soil according to Cd tolerance of wheat, and 2 kg of Cd-laden soil was filled in plastic pot (16.2 cm diameter, 23.5 cm height). To mimic emergent remediation by applying DGB immediately after Cd entering soil, DGB was evenly amended in Cd-laden soil at low (2%, w/w) and high rate (4%, w/w), respectively, according to actual biochar-amendment rates in farmland soils (Li et al. 2011; Aamer et al., 2020). Thus, fresh DGB-amended soil was obtained. To obtain aged DGB-amended soil, DGB was kept in Cd-laden soil for 6 months at 25 °C and carefully retrieved by forceps for aged DGB characterization.

Differently amended soils were termed as low rate-biochar Cd soil (LBCd), high rate-biochar Cd soil (HBCd), LBCd + 6 and HBCd + 6, respectively, based on DGB rate (low, high) and aging time (6 months). Cd-laden soil without DGB was control soil (i.e., CONCd).

Pot experiments were done in greenhouse at west campus of China Agricultural University. Each amended soil was obtained simultaneously to ensure that all pot experiments commenced concurrently. Pot system for amended and control soils was run in triplicate, where 0.5 g of urea was applied. All soils were moistened at 60% of water-holding capacity to mimic farmland soil moisture. Five seeds of wheat (*Triticum aestivum* L.) cultivar 'Aikang 58' were sowed per pot and after sprouting three seedlings continued to grow for 60 days, during which water loss from soil was compensated by deionized water.

2.3 Wheat Growth and Cd Uptake Analyses

At harvest, leaf chlorophyll content was directly monitored by chlorophyll meter (Yaxin-1260, China). The whole wheat was retrieved and roots were gently swept using brush to retrieve rhizospheric soil that immediately stored at –80 °C for further test. Wheat height was recorded to characterize growth. To clarify Cd uptake, wheat sample was separated into such four parts as roots, stems, leaves, and grains, which were rinsed by deionized water and oven-dried at 105 °C. Cd in each part was quantified by inductively coupled plasma optical emission spectrometer (ICP-OES) (Agilent 5110, USA) after microwave digestion with HNO_3 at 1000 W and 180 °C for 30 min.

2.4 Soil Characterization and Soil Cd Fractions Analyses

At harvest, DGB-amended and control soils were air-dried and characterized by procedures in Supplementary Information. Three-stage sequential fractionation procedure proposed by European Community Bureau of Reference was used to extract acid-soluble, reducible, oxidizable, and residual fractions of soil Cd (Supplementary Information). The procedure was repeated thrice for each soil. After each fractionation, mixture was centrifuged to retrieve supernatant. Residue was washed by deionized water, and the washings were combined with the supernatant. The residue was then used for next fractionation step. Each Cd fraction was detected by ICP-OES (Agilent 5110, USA).

2.5 Rhizospheric Bacterial Composition Analysis

Rhizospheric soil DNA from triplicate sample was extracted by DNeasy PowerSoil kit (Qiagen, Germany) and pooled. DNA purity and quantity were verified by spectrophotometer (NanoDrop Technologies, USA). V3–V4 region of bacterial 16S rRNA was PCR-amplified with primers 343F (5′-TAC GGRAGGCAGCAG-3′) and 798R (5′-AGGGTATCTAAT CCT-3′). Detail PCR protocol, product purification, and quantification procedures were described in Supplementary Information.

High-throughput paired-end (2×300 bp) sequencing was run on Illumina Miseq platform. Raw sequencing data were trimmed by discarding primer sequences by Cutadapt (1.18). Paired-end reads were assembled using PEAR (0.9.8) and filtered by removing sequences with quality scores < 20 using PRINSEQ (0.20.4). High-quality reads were clustered into operational taxonomic units (OTUs) at 97% similarity threshold. Heatmap analysis was run based on Kyoto Encyclopedia of Genes and Genomes (KEGG) level 2. Clustering correlation heatmap was generated using R with gplots package (3.0.1.1). Linear discriminant analysis Effect Size (LEfSe) was run with LEfSe (1.1.0) to discern differently abundant taxa among different rhizospheric soils. Redundancy analysis (RDA) was run by Canoco (5.0) to examine the relationship between soil properties and bacterial composition. Significance, high significance and extremely high significance was assigned at $p < 0.05$, $p < 0.01$, and $p < 0.001$, respectively.

2.6 Statistical Analysis

One-way analysis of variance with Duncan's multiple comparison was conducted using SPSS software (26.0) to determine statistically significant difference among treatments at $p < 0.05$.

3 Results

3.1 Fresh and Aged DGBs Characterization

After aging in Cd-laden soil, DGB had more abundant O but lower C content (Table 1), because labile organic fractions could be decomposed during aging to decrease C content while oxidation during aging could generate oxygenic groups to increase O content. Thus, aged DGB showed higher O/C value that denoted higher aromaticity, while fresh DGB had lower aromaticity and thus lower biochemical stability. K and Si drove soil cation exchange to regulate HMs sorption. Compared to fresh DGB, aged DGB had higher K but lower Si content and had smaller SSA, total pore volume, and average pore size, thus aging in soil destroyed DGB's porous structure (Table 1). Obeying SSA and porosity data, SEM results showed that fresh DGB had developed porosity, where pore channels were intact and clear to well form porous structure, whereas porous structure of aged DGB was mostly destroyed with rougher surface (Fig. 1).

Table 1 Element composition, specific surface area (SSA) and porosity of fresh and aged distiller's grain-derived biochar (DGB)

	C	N	O	K	Si	O/C*	SSA $(m^2\ g^{-1})$	Total pore volume $(cm^3\ g^{-1})$	Average pore size (nm)
Fresh DGB	60.3%	0.09%	21.56%	0.45%	17.6%	35.75	5.3774	0.0198	14.7283
Aged DGB	40.33%	2.51%	39.91%	1.74%	8.95%	98.96	3.7273	0.0091	9.6734

*Higher O/C value denotes higher aromaticity (Spokas 2010; Li et al. 2018)
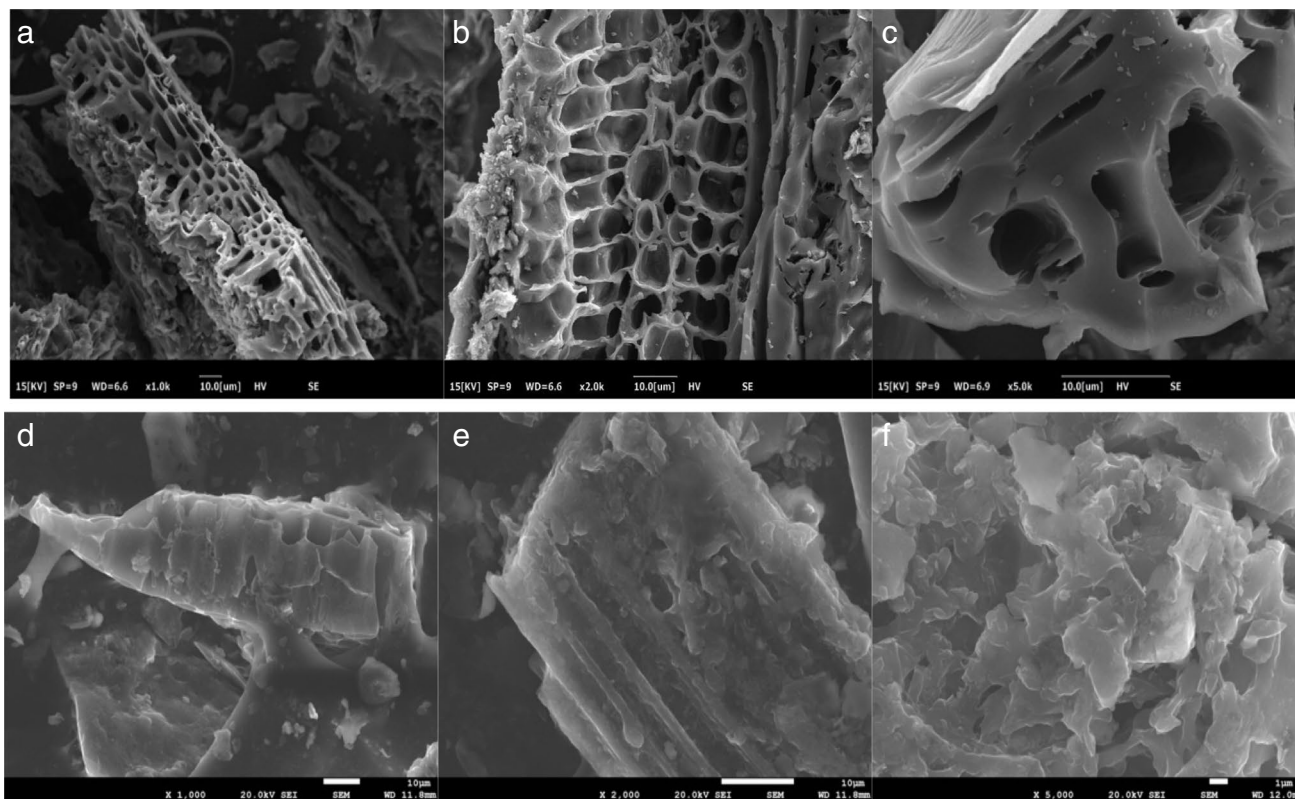
Fig. 1 The morphology of fresh distiller's grain-derived biochar (DGB) ($\mathbf{a}, \times 1000$; $\mathbf{b}, \times 2000$; $\mathbf{c}, \times 5000$) and aged DGB ($\mathbf{d}, \times 1000$; $\mathbf{e}, \times 2000$; $\mathbf{f}, \times 5000$)

The functionality of DGB was identified by FTIR (Fig. 2). Judged from peak intensity at 1089 cm^{-1} that represented aliphatic C-O stretching, both fresh and aged DGBs had abundant C-O group because DGs were rich in cellulose, hemicellulose, and sugar. The peak at 1584 and 805.24 cm^{-1} resulted from aromatic C=C stretching and aromatic C-H bending wagging, respectively (Fig. 2). Aged DGB had stronger intensity of these peaks than fresh DGB, thus aging process induced production of aromatic structure, which obeyed O/C value verified by element analysis (Fig. 2, Table 1). Correspondingly, the peak at 2921.72 cm^{-1} representing aliphatic or cycloparaffin C-H stretching disappeared (Fig. 2). The peak intensity at 3300–3600 cm^{-1} denoted -OH group stretching, which was crucial for Cd passivation via Cd-ligands coordination bonds.

3.2 Fresh and Aged DGB-Amended Soil Characterization

Compared to control soil (CONCd), the pH of 2% DGB-amended soil (LBCd) and 4% DGB-amended soil (HBCd) increased from 7.72 to 7.82 and to 7.91, respectively, yet soil pH slightly dropped after 6-month aging. Concretely, the pH of LBCd + 6 and HBCd + 6 decreased by 3.66% and 1.54%, respectively (Table 1). Likewise, soil organic matter (SOM) content increased by 6.80 and 11.08 times at 2% and 4% DGB amendment, respectively, but slightly dropped by 17.53% and 16.15% at 2% and 4% DGB amendment after aging, which still exceeded CONCd. Total carbon (TC) content in soil also increased from 4.34 to 16.53 and 21.83 g kg^{-1} at 2% and 4% DGB amendment, respectively,
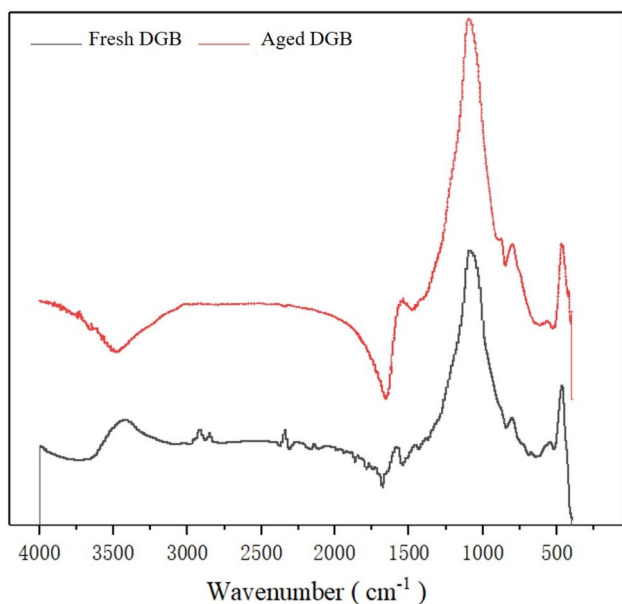
Fig. 2 Fourier transform infrared (FTIR) spectra of fresh DGB and aged DGB

but declined to 12.16 and 17.97 g kg^{-1} at 2% and 4% DGB amendment after aging (Table 1).

In comparison, total nitrogen (TN) content increased from 0.27 to 0.63 and 1.03 g kg^{-1} at 2% and 4% DGB amendment, respectively, and continuously elevated after aging. At 2% and 4% DGB amendment, available K content increased by 133.71% and 172.27%, respectively, and continuously elevated by 5.22% and 0.31%, respectively, after aging (Table 1). Contrarily, NO_3-N content largely decreased after DGB amendment compared to CONCd (Table 1), likely because DGB suppressed nitrifier abundance but promoted more N accumulation as NH_4-N for wheat assimilation.

3.3 Wheat Growth and Cd Uptake

DGB significantly increased wheat growth and relative chlorophyll content (soil–plant analyzer development (SPAD) index). Specifically, 2% and 4% DGB amendment increased wheat height by 25.67 and 22.57 cm, respectively, and increased relative chlorophyll content by 27.87% and 80.46%, respectively, compared to CONCd (Fig. 3). This was because DGB amendment raised soil nutrient content and improved K and TN sequestration (Table 1). Yet, wheat growth and chlorophyll content somewhat dropped after aging. At 2% and 4% DGB amendment, wheat height dropped by 35.33% and 11.58%, respectively, and chlorophyll content dropped by 3.09% and 8.20%, respectively, after aging compared to those without aging, but height and relative chlorophyll content after aging still exceeded CONCd (Fig. 3).

DGB amendment generally decreased Cd content in wheat roots, stems, leaves, and grains (Fig. 4). Compared to CONCd, Cd content in roots decreased by 23.17% and 42.97%, respectively, and further decreased by 6.65% and 2.66% after aging, respectively, at 2% and 4% DGB amendment (Fig. 4a). Cd content in leaves decreased by 0.65% and 31.60%, respectively, and further decreased by 7.54% and 28.90% after aging, respectively, at 2% and 4% DGB amendment (Fig. 4b). Cd content in stems decreased by 6.91% and 6.91%, respectively, and further decreased by 45.54% and 60.74% after aging, respectively, at 2% and 4% DGB amendment (Fig. 4c). Cd content in grains decreased by 15.49% and 26.06%, respectively, without apparent change after aging at 2% and 4% DGB amendment (Fig. 4d).

3.4 Soil Cd Fraction Distribution

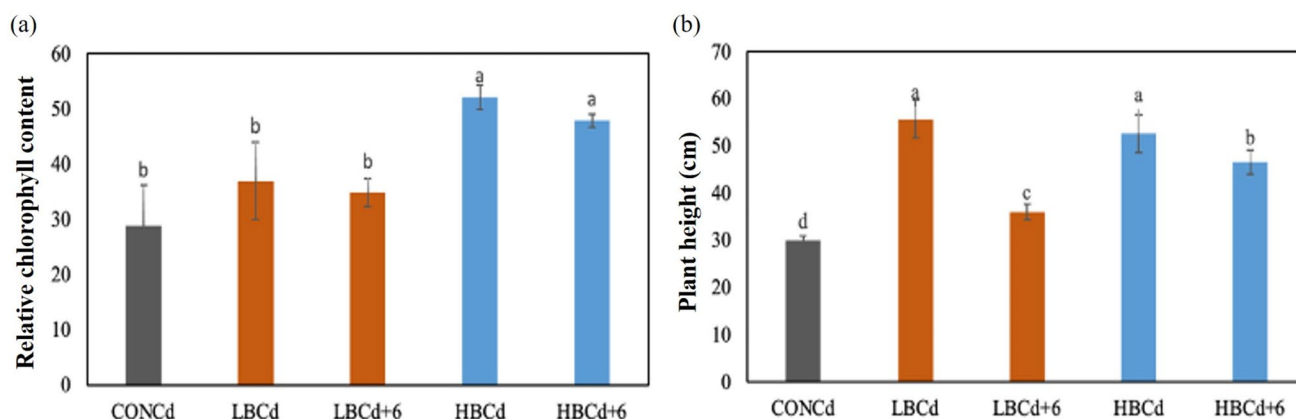DGB amendment altered Cd fractions distribution in soil. Concretely, the proportion of acid-soluble Cd decreased

Fig. 3 Relative chlorophyll content (**a**) and height (**b**) of wheat in different treatments. Mean and standard error (SE) of triplicate are shown as bar. Different letters indicate significant ($p < 0.05$) difference in means among different treatments
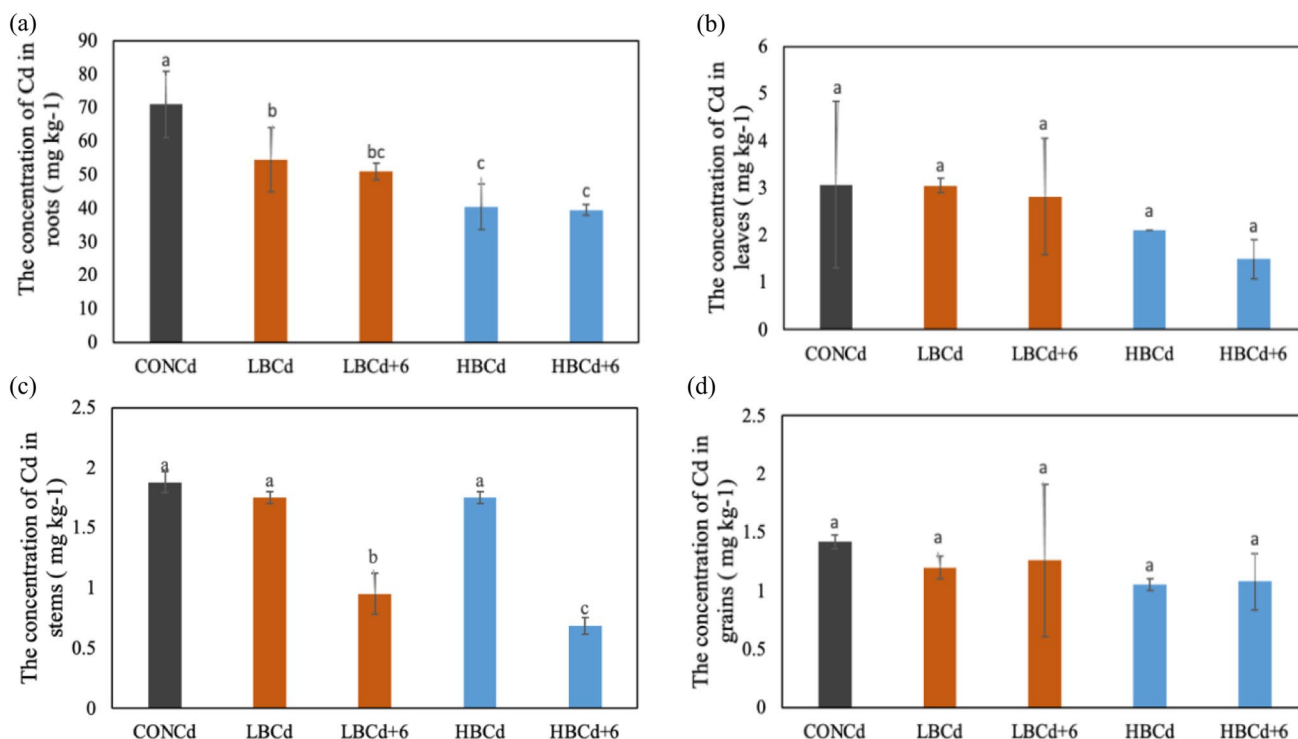
Fig. 4 Cd content in roots (**a**), leaves (**b**), stems (**c**), and grains (**d**) of wheat in different treatments. Mean and standard error (SE) of triplicate are shown as bar. Different letters indicate significant ($p < 0.05$) difference in means among different treatments

from 91% to 83% and 71% at 2% and 4% DGB amendment, respectively. After aging, acid-soluble Cd increased to 89% at 2% DGB amendment, which was still lower than CONCd, yet acid-soluble Cd sharply declined to 48% at 4% DGB amendment (Fig. 5). Thus, acid-soluble Cd fraction in soil progressively decreased as DGB rate increased (Fig. 5). Contrarily, soil residual Cd fraction continuously increased as DGB rate increased and aging proceeded. The proportion of residual Cd fraction did not change but after aging residual Cd increased to 3% at 2% DGB amendment, while at 4% DGB amendment the residual Cd increased to 6% and further elevated up to 18% after aging, compared to CONCd (Fig. 5). Soil reducible Cd decreased from 7% to 8% and 33% after aging at 2% and 4% DGB amendment, respectively, and soil oxidizable Cd fraction did not change obviously at DGB amendment (Fig. 5). Soil acid-soluble and residual Cd fraction contents implied that wheat had lower Cd-absorbing capability at higher-rate (4%) DGB amendment, especially after aging, agreeing to the result of Cd uptake by each wheat part (Fig. 4).

3.5 Rhizospheric Bacterial Composition

Generally, 2485 OTUs were shared among different treatments (i.e., CONCd, LBCd, LBCd + 6, HBCd, HBCd + 6) (Fig. S1). Compared to CONCd, no significant difference

existed in OTU number between LBCd and HBCd (5799 vs. 5819), but after aging OTU number of LBCd and HBCd declined to 5127 and 4527, respectively, indicating that biodiversity sharply decreased after aging, coincided with Chao index result (Fig. 6a, S1). Shannon and Simpson index can evaluate alpha-diversity in community. After aging, Shannon index obviously decreased, signifying decreased biodiversity. Similar result was reflected by Simpson index (Fig. 6b, c). Figure 6d depicted that sequencing depth here was enough to highly cover overall composition of each treatment, so sequencing data were reliable for downstream analyses.

Bacterial composition at each taxonomic level was illustrated in Fig. 7, with the height of each color square in column representing the abundance of each group in community. At phylum level, dominant groups were Proteobacteria, Actinobacteria, and Bacteroidetes, whose abundance totally occupied nearly 80% in each treatment (Fig. 7a). Compared to CONCd, DGB amendment increased Actinobacteria and decreased Proteobacteria abundance. After aging, Actinobacteria abundance continued to increase but Proteobacteria abundance continuously decreased. Besides, the abundance of Acidobacteria, Nitrspirae, Elusimicrobia, and Latescibateria phyla declined as DGB rate increased and aging proceeded, while Verrucomicrobia abundance was not significantly affected by DGB rate but increased as aging proceeded, and Cyanobacteria increased with rising rate and
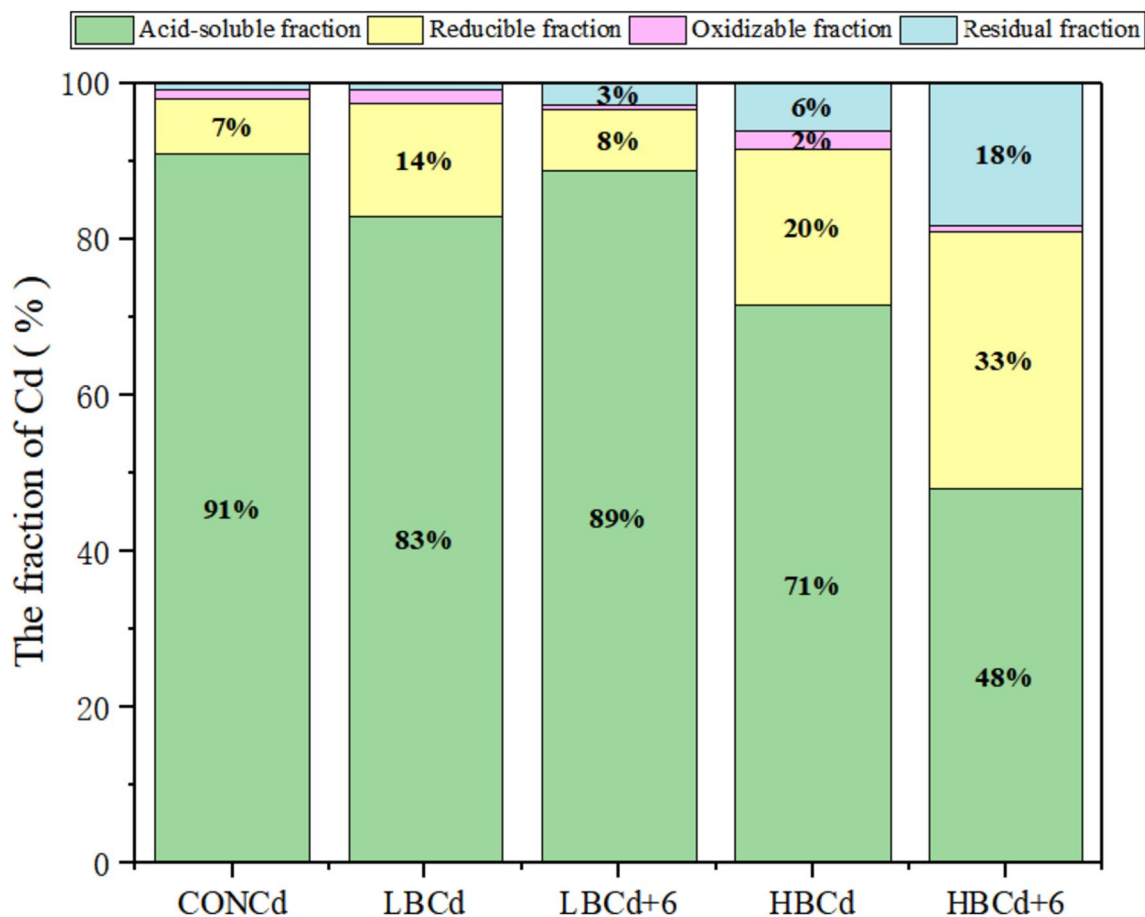
Fig. 5 Proportion of soil Cd fractions in different treatments

aging (Fig. 7a). LEfSe analysis verified that Actinobacteria and Acidobacteria were the discriminant phyla among different treatments, especially Acidobacteria abundance in CONCd and Actinobacteria abundance in HBCd + 6 significantly exceeded that in other treatments (Fig. 8).

At order level, Cytophagales and Microtrichales abundance increased, while Myxococales and Betaproteobacteriales abundance decreased as DGB rate increased. As aging proceeded, Cytophagales, Propionibacteriales, Micrococcales, and Microtrichales increased, but Myococcales showed decrease trend (Fig. 7b). At family level, with rising DGB rate, Microscillaceae and Nocardioidaceae abundance increased, but Haliangiaceae, TRA3-20, Gaiellaceae, Nitrospiraceae, and Nitrosomonadaceae decreased. As aging proceeded, Microscillaceae and Nocardioidaceae increased, but Haliangiaceae, Nitrosomonadaceae, and Alteromonadaceae showed decrease trend (Fig. 7c). Four orders (Cytophagales, Betaproteobacteriales, Propionibacteriales, Micrococcales) and four families (Nocardioidaceae, Nitrosomonadaceae, Microscillaceae, Micrococcaceae) were identified as discriminant groups among different treatments (Fig. 8). Particularly, abundance of Nitrosomonadaceae (belonging to

Betaproteobacteriales order) in CONCd and Nocardioidaceae (belonging to Propionibacteriales order), Microscillaceae (belonging to Cytophagales order), and Micrococcaceae (belonging to Micrococcales order) in HBCd + 6 significantly exceeded other treatments (Fig. 8).

At genus level, *MND1* and *Sphingomonas* decreased with rising DGB rate, and *Nitrospira* and *Haliangium* decreased as aging proceeded. *Marmoricola*, *Lysobacter*, *Pseudarthrobacter*, and *Massilia* increased with rising DGB rate and aging process (Fig. 9). Three identified genera (*Nocardioides*, *Pseudarthrobacter*, *MND1*) were discriminant genera among different treatments, where *MND1* (belonging to Nitrosomonadaceae family) abundance in LBCd, *Nocardioides* (belonging to Nocardioidaceae family) and *Pseudarthrobacter* (belonging to Micrococcaceae family) abundances in HBCd + 6 were significantly higher than other treatments (Fig. 8).

Based on above data, DGB amendment here altered soil fertility and Cd bioavailability and thus changed dominant groups abundance at each taxonomic level, but significant abundance changes of several dominant groups were mostly observed in HBCd + 6 (Figs. 7 and 8).
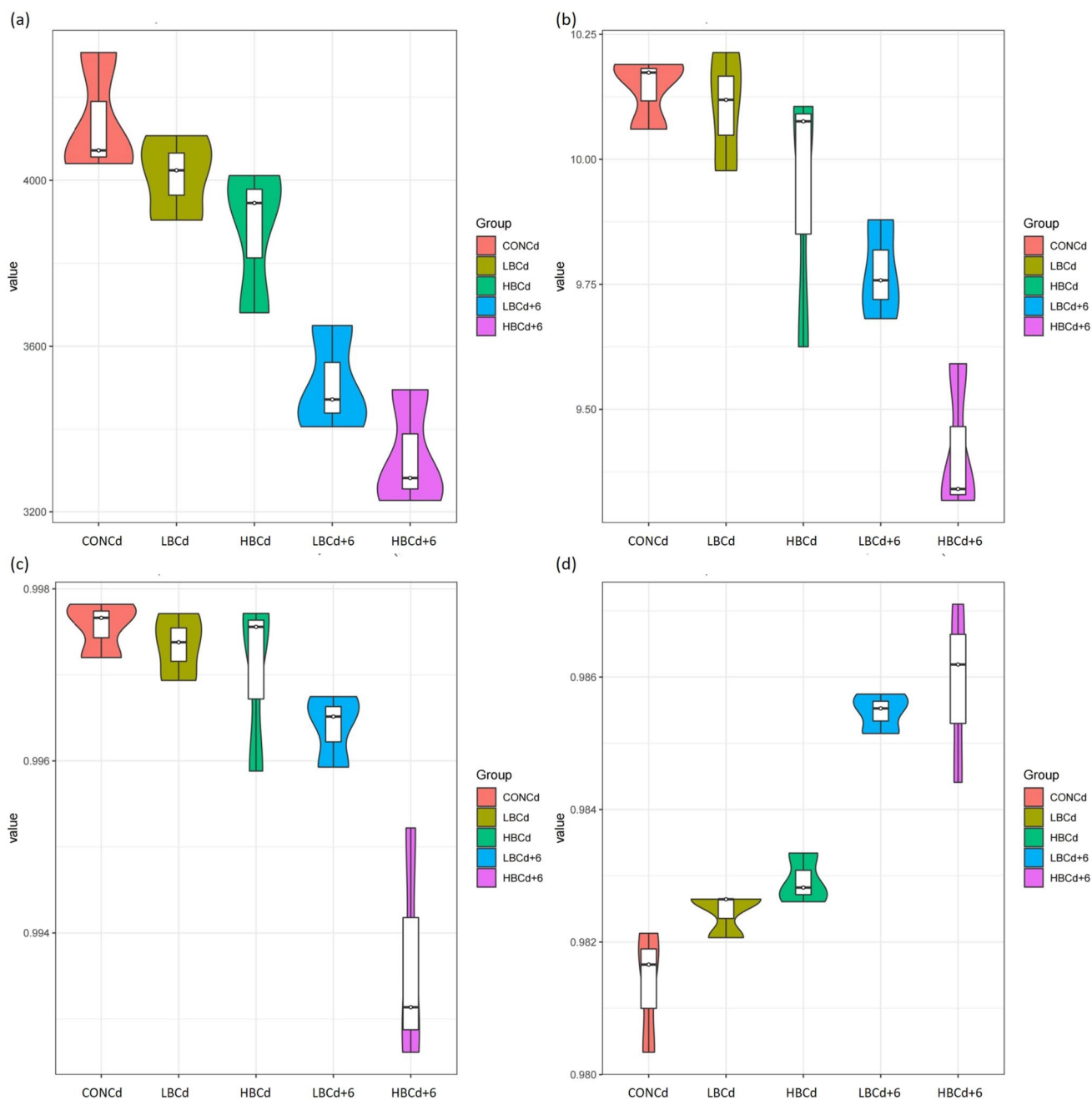
Fig. 6 Alpha-diversity indices, including Chao (**a**), Shannon (**b**) and Simpson (**c**) index, and sequencing coverage (**d**) for rhizospheric bacterial composition in different treatments

4 Discussion

Converting DGs into DGB as soil amendment is a reasonable option for soil Cd-immobilization and agro-food risk mitigation, which was a promising development direction that promotes DGs' recycling and added value of brewing industry, but almost no attempt focused on this issue. Besides, natural aging effects of DGB at different amendment rates on wheat growth and Cd uptake, soil Cd fractions distribution, and soil nutrient content still remained unclear, and in particular how rhizospheric microbiota changed as response to DGB amendment with aging process in Cd-laden soil was unknown. To address above gaps, this study converted DGs into DGB to promote Cd-immobilization and wheat growth in Cd-laden soil and elucidate underlying mechanisms from the perspective of Cd uptake, soil nutrient and Cd bioavailability, and rhizospheric bacterial composition. Results revealed that natural aging in soil increased K
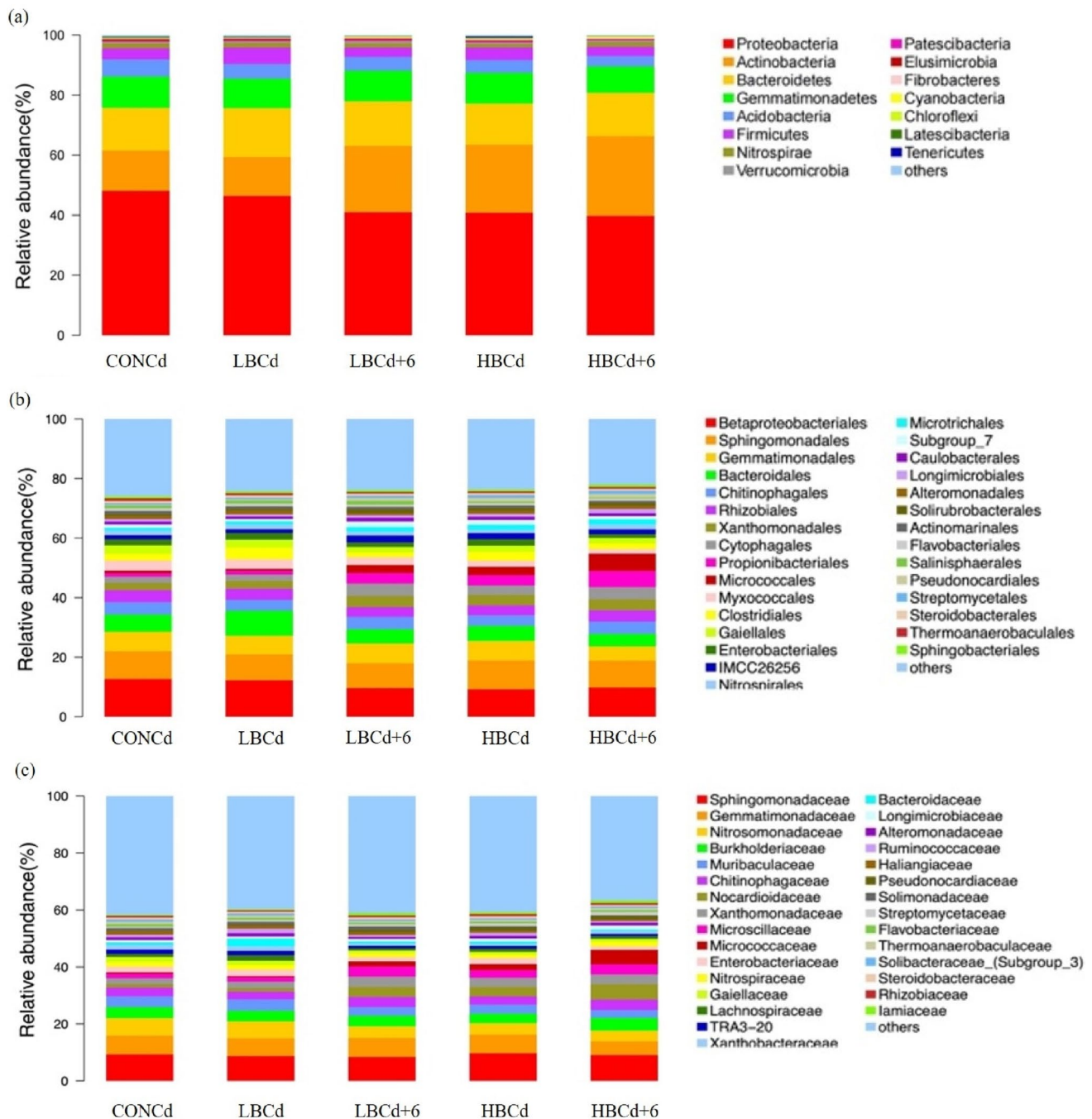
Fig. 7 Rhizospheric bacterial composition at phylum level (**a**) (with the top 15 most abundant groups shown) and at order (**b**), and family (**c**) level (with the top 30 most abundant groups shown) in different treatments. The height of each color square in column represents the relative abundance of each group

but decreased Si content of DGB (Table 1), implying that Si could be released into soil during aging to combine with soil Cd and form Si-Cd composites for preventing Cd translocation through roots and decreasing Cd transport-related gene expression (Wang et al. 2020b; Khan et al. 2021). Aging also destroyed DGB's porous structure (Fig. 1, Table 1), likely because soil microbes and organic particles filled and

blocked pores, and organic matter biodegradation might also break intact porous structure (Martin et al. 2012; Yuan et al. 2021c). Since DGB's porous structure was destroyed after aging, thus O and/or H atoms could be adsorbed onto broken pores during aging to form oxygenic groups (Mukherjee et al. 2011). The increased oxygenic groups (e.g., -OH, C-O) could also result from oxidation during
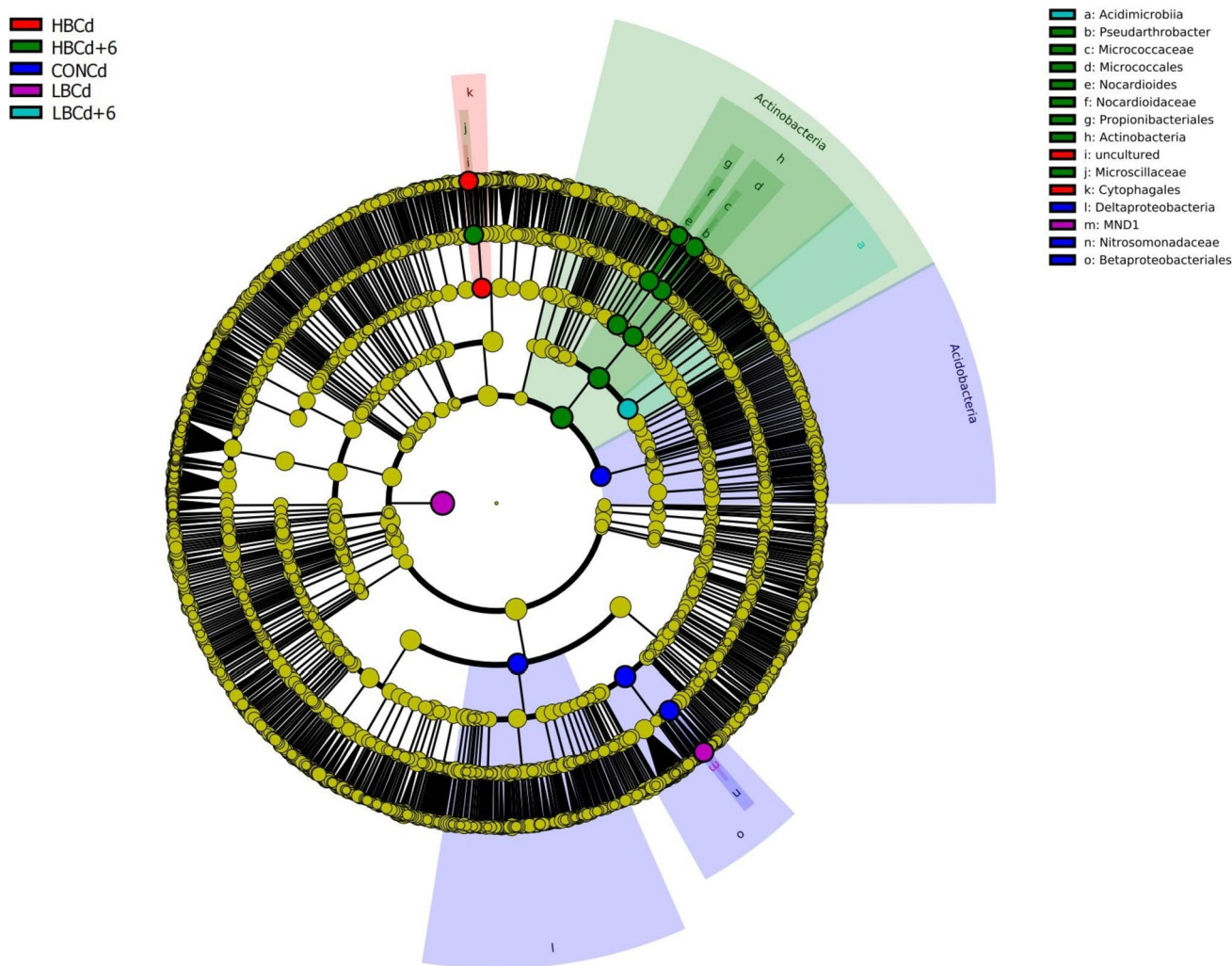
Fig. 8 Taxonomic differences of rhizospheric bacterial composition at phylum, class, order, family, and genus levels among different treatments based on Linear discriminant analysis Effect Size (LEfSe)

aging, which declined HMs' bioavailability and mobility via forming stable HM-complexes/precipitates (Fan et al. 2018; Gao et al. 2019).

Soil pH more greatly increased with rising DGB rate, but slightly dropped after 6-month aging (Table 2). Increased soil pH at DGB amendment was due to inherent alkalinity of DGB that can increase surface alkali groups in soil, but extensive oxidation during aging could enhance surface acidity by generating oxygenic groups (e.g., carboxyl, hydroxyl) to decrease soil pH after aging (Mukherjee et al. 2014; Yuan et al. 2021c). New carbonate formed by adsorbing CO_2 and low-molecular-weight organic acid decomposed from organic carbon of DGB during aging process could also decrease soil pH (Yao et al. 2010; Xu et al. 2016). Moreover, rising DGB rate more strongly increased soil TC, TN, available K, and SOM to promote wheat growth and relative chlorophyll content, while 6-month aging further

increased soil TN and available K content but slightly dropped SOM and TC content (Table 2). These indicated that higher DGB rate more greatly improved soil nutrient and fertility, regardless of fresh and aged DGB. Thus, DGB as soil amendment enhanced soil nutrient sequestration to avoid nutrients loss, similar to Jabbrova et al. (2023) where biochar promoted crop growth by raising soil nutrient availability. Yet, aging impeded the further increase of SOM and TC contents, mostly because SOM could be decomposed with some carbohydrates being degraded into inorganic compounds during aging (Yuan et al. 2021d). Contrary to SOM and TC trends, TN and available K content continuously increased as aging proceeded. One reason was that DGB could bind to elements adsorbed on pore surface, especially aged DGB with increased oxygenic groups (e.g., -OH, C-O) could form H-bond with N-containing ions, thus enhancing TN sequestration (Luo et al. 2021). Besides K
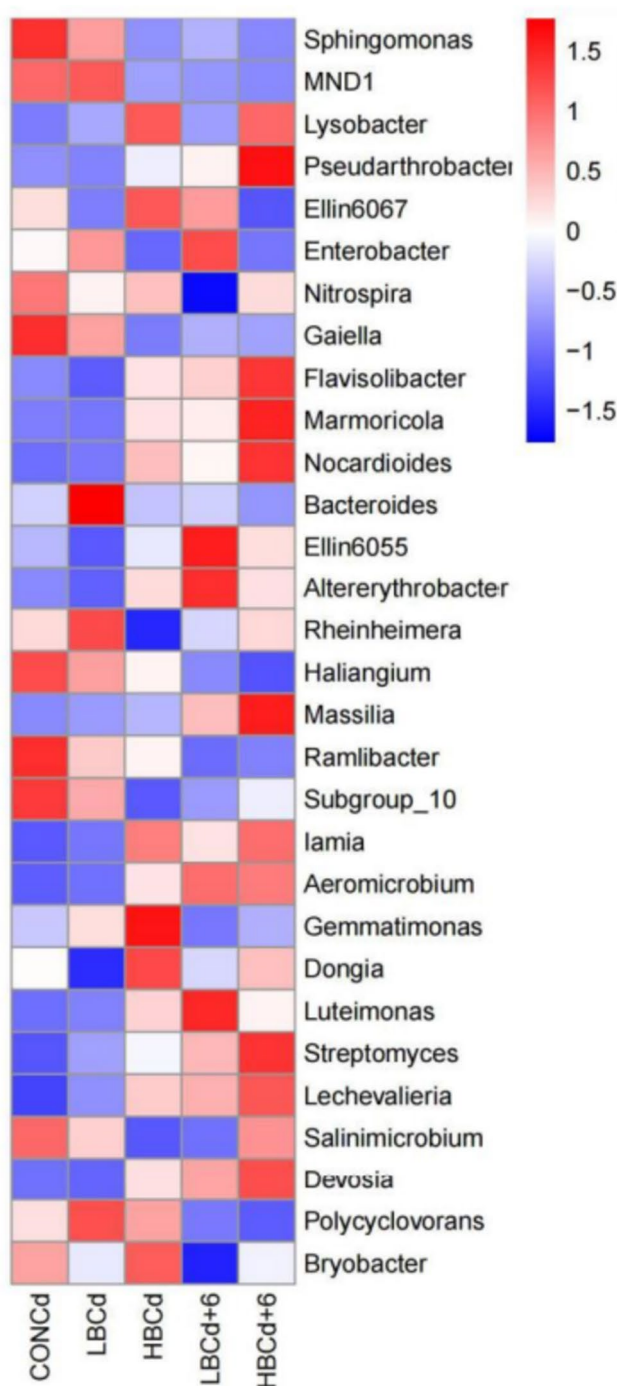
Fig. 9 Heatmap of rhizospheric bacterial composition at genus level (with the top 30 most abundant genera shown) in different treatments. The red in color bar represents higher relative abundance and blue indicates lower relative abundance

release from DGB, complex biochemical conversion and stimulated microbial activity might cause the continuously increased available K content along aging process (Basak et al. 2022). Overall, SOM content and pH dropped after aging due to organic fraction decomposition and oxygenic

groups generated, while aging process further sequestrated soil TN and available K to avoid their losses.

Contrarily, soil NO_3-N content more strongly decreased with rising DGB rate and further decreased with aging process (Table 2). Nitrification is a process where microbes oxidize NH_4-N to NO_2-N and NO_3-N and included two stages: the first is ammonia oxidation stage mainly initiated by ammonia-oxidizers, and the second is nitrite oxidation stage (Norton and Stark 2011). The nitrifier abundances of Nitrosomonadaceae and Nitrospiraceae more largely decreased with rising DGB rate and aging process (Fig. 7c). This suggested that rising DGB rate tended to inhibit nitrification but enhance N-fixation, thus explaining the reason for continuously decreased NO_3-N but increased TN content along aging at each DGB rate (Table 2). Likewise, Yao et al. (2022) revealed that wheat straw-derived biochar amendment inhibited soil nitrification by shifting the community structure and decreasing the abundance of ammonia-oxidizers. Moreover, rising DGB rate more sharply increased N-fixer *Ensifer_meliloti* abundance, which might also be responsible for increased NH_4-N with rising DGB rate (Table S2).

Previous studies observed declining Cd uptake by plant roots, stems, and/or grains with rising amendment rate (Bashir et al. 2018; Akca et al. 2023; Usman et al. 2023). This study verified that rising DGB rate more sharply decreased Cd uptake by each part of wheat, and Cd content in each part was negatively related to DGB rate (Fig. 4) and further surveyed aging effect of different DGB rates on Cd uptake by each wheat part. Results innovatively showed that 6-month aging tended to further decrease Cd uptake by wheat roots, stems, and leaves and did not obviously change Cd uptake by wheat grains, which is edible part for consumption (Fig. 4). This involved the re-distribution of soil Cd fractions after DGB amendment with aging process. Here, residual Cd fraction increased with rising DGB rate and aging process, implying that higher-rate DGB elicited stronger Cd passivation than lower-rate DGB, likely because high-rate DGB caused greater electrostatic force and surface sorption to form complexation and/or precipitation that promoted soil Cd passivation. As aging proceeded, more oxygenic acidic groups were generated to render DGB more negatively charged by ionization and deprotonation, thus enhancing electrostatic attraction to cationic Cd. Meanwhile, Si was released from DGB during aging to form stable Cd-composites/precipitates and thus further increased residual Cd fraction to promote Cd passivation (Fig. 2, Table 1). Cheng et al. (2020) proposed that NO_3-N addition promoted Cd accumulation in wheat roots, regardless of soil NH_4-N level. From this view, DGB amendment here decreased soil NO_3-N and after aging NO_3-N further decreased, thus blocking Cd accumulation in wheat roots. Above effects decreased Cd uptake by

Table 2 Key soil parameters reflecting nutrient content of different treatments

Treatment	pH	Soil organic matter (SOM, g kg⁻¹)	Total carbon (TC, g kg⁻¹)	Total nitrogen (TN, g kg⁻¹)	NH₄-N (mg kg⁻¹)	NO₃-N (mg kg⁻¹)	Available K (mg kg⁻¹)
CONCd	7.72 ± 0.02 ab*	2.61 ± 0.68 c	4.34 ± 0.38 d	0.27 ± 0.01 c	0.23 ± 0.05 b	1.35 ± 0.96 a	48.21 ± 2.28 c
LBCd	7.82 ± 0.02 ab	17.74 ± 5.65 b	16.53 ± 3.75 b	0.63 ± 0.15 b	0.97 ± 0.03 a	0.69 ± 0.15 ab	112.67 ± 12.19 b
LBCd+6	7.70 ± 0.17 ab	14.63 ± 1.75 b	12.16 ± 0.46 c	0.76 ± 0.04 b	0.22 ± 0.11 b	0.66 ± 0.36 ab	118.55 ± 3.61 ab
HBCd	7.91 ± 0.20 a	28.92 ± 1.91 a	21.83 ± 0.70 a	1.03 ± 0.23 a	1.02 ± 0.04 a	0.84 ± 0.42 ab	131.26 ± 8.77 a
HBCd+6	7.63 ± 0.05 b	24.25 ± 3.92 a	17.97 ± 0.87 b	1.18 ± 0.17 a	0.16 ± 0.03 b	0.26 ± 0.09 b	131.66 ± 3.32 a

*Mean and standard error of triplicate are shown. Different letters indicate significant ($p < 0.05$) difference in means among different treatments

wheat and interrupting Cd transfer in soil-wheat system (Fig. 5). Besides, soil pH might induce increased residual Cd. Previous studies proposed that rising pH caused by biochar-amendment facilitated oxygenic group dissociation to induce soil Cd stabilization (Houben and Sonnet 2015; Wang et al. 2018). However, soil pH increase caused by biochar-amendment was time-limited, partly due to alkali metal-leaching from biochar (Shi et al. 2019; Gao et al. 2020). This study observed that soil pH increased at DGB amendment but somewhat dropped after aging, thus soil pH was not crucial factor for continuously increased residual Cd content as aging proceeded. Consequently, the mechanisms by which rising DGB rate and aging process affected wheat growth and Cd uptake involved the increased soil nutrient content (SOM, TC, TN, NH₄-N, available K) and decreased soil Cd bioavailability (Figs. 4, 5, Table 2). Considering improved soil fertility, decreased Cd bioavailability, promoted growth, and decreased Cd uptake of wheat, 4% DGB rate with 6-month aging could be suitable DGB-amending scheme for promoting soil fertility and blocking Cd-induced risk in soil.

RDA was conducted to reveal the correlation between soil Cd fractions, nutrient contents, and bacterial composition. At phylum and genus level, both axes (RDA1, RDA2) jointly explained 76.9% and 58.3% of total variation in Cd fractions, nutrient contents, and bacterial composition, respectively, indicating a critical influence between soil Cd fractions, nutrient contents, and bacterial composition variation (Fig. 10). Residual Cd fraction had positive correlation with soil TN, SOM, TC, and available K content, but negative correlation with soil NH₄-N content. Acid-soluble Cd fraction was positively correlated to NH₄-N and NO₃-N content, but negatively to TN, SOM, TC, and available K content (Fig. 10). Thus, improved soil fertility at DGB amendment was closely related to fractions re-distribution. Furthermore, three treatments as HBCd+6, HBCd, and LBCd+6 were positively correlated to TN, SOM, TC, available K, and residual Cd content. Consequently, both factors of DGB rate and aging statistically involved soil fertility improvement and Cd conversion into residual fraction (Fig. 10).

Rhizospheric bacterial composition could also contribute to soil fertility change and Cd fractions re-distribution. At
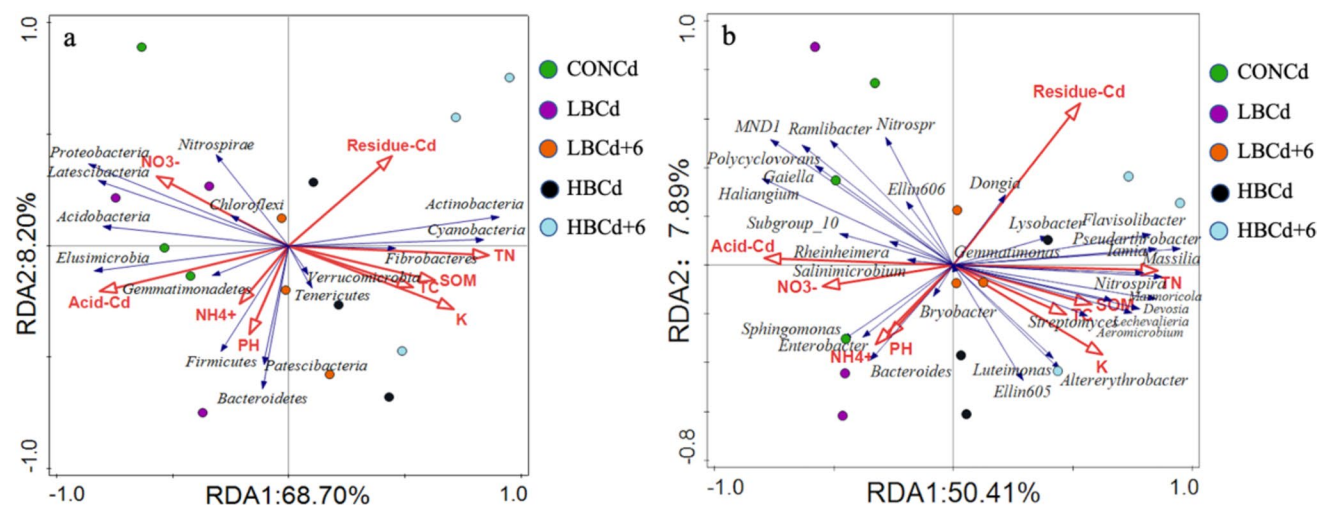

Fig. 10 Redundancy analysis (RDA) for correlations between soil nutrients/Cd fractions and rhizospheric bacterial composition at phylum (**a**) and genus (**b**) level among different treatments

phylum level, DGB amendment increased Actinobacteria but decreased Proteobacteria abundance, and after aging Actinobacteria abundance increase and Proteobacteria abundance decrease continued (Fig. 7a). Actinobacteria phylum included many members with high metabolic ability and bioremediation potential (Alvarez et al. 2017). Proteobacteria, as a common phylum in soil and sediment, acted as a large population with strong Cd-tolerance in HM-laden soil, and its abundance was also related to HM-removal (Gillan et al. 2005; Kuppusamy et al. 2016; Yu et al. 2021; Zuo et al. 2023). Effect of HMs on soil bacterial composition mainly depended on soil HMs bioavailability (Alvarenga et al. 2008). Here, decreased Proteobacteria and increased Actinobacteria abundance after DGB amendment with aging process accorded with decreased soil Cd bioavailability and promoted Cd passivation after DGB amendment and aging (Fig. 5). As verified statistically, obvious positive correlation existed between Actinobacteria, Cyanobacteria, and Fibrobacteria abundance and residual Cd, TN, SOM, TC, and available K content, while Proteobacteria, Acidobacteria, Elusimicobia, Latescibacteria, and Nitrospirae abundance negatively correlated to residual Cd, TN, SOM, TC, and available K content. Acid-soluble Cd fraction was positively correlated to Proteobacteria, Nitrospirae, Latescibacteria, Elusimicobia, Gemmatimonadetes, and Acidobacteria abundance (Fig. 10a). At genus level, *Marmoricola*, *Lysobacter*, *Pseudarthrobacter*, and *Massilia* increased with rising DGB rate and aging process (Fig. 9). Among these genera, *Lysobacter* members are biocontrol bacteria antagonistic against diverse plant pathogens and commonly inhabit plant rhizosphere. Involvement of *Lysobacter* in controlling plant pathogens could be sustained by its ability to prey on other microbes through 'wolf-pack behavior' and to produce various lytic enzymes and bioactive metabolites (Seccareccia et al. 2015; Puopolo et al. 2018). Presence of *Lysobacter* members in croplands was often related to suppression of soil pathogenic microbes (Bacosa and Inoue 2015). Here, *Lysobacter* abundance increased with rising DGB rate and aging process, thus aged DGB amendment tended to improve soil resistance to various pathogens. *Massilia* belonging to *Betaproteobacteria* was another key rhizospheric genus that can secret multiple metabolites/enzymes, solubilize phosphorus, degrade phenanthrene, and resist HMs (Zheng et al. 2017; Yang et al. 2020). Wang et al. (2020a) identified a mercury-tolerator as *Massilia* and found increased *Massilia* tolerance and abundance with increasing mercury level. Here, increased *Massilia* abundance could reflect enhanced P bioavailability and bioactive metabolites contents with rising DGB rate and aging process. RDA verified that *Lysobacter* and *Massilia* abundance, together with *Pseudarthrobacter*, *Iamia*, *Nitrospira*, *Flavisolibacter*, *Devosia*, and *Marmoricola* abundance, were positively correlated to residual Cd, TN, SOM, TC, and available K content, but acid-soluble Cd fraction was positively correlated to *MND1*,

Sphingomonas, *Haliangium*, and *Enterobacter* abundance (Fig. 10b). According to RDA result, rising DGB rate and DGB aging jointly increased the abundances of Actinobacteria, Cyanobacteria, Fibrobacteria phyla, and *Lysobacter*, *Massilia*, *Pseudarthrobacter*, and *Iamia* genera. Thus, close correlation existed between DGB rate, DGB aging, and dominant groups abundance (Fig. 10). Particularly, higher rate (4%) DGB with aging process led to significant change in bacterial composition and soil nutrient/Cd bioavailability.

Spearman correlation analysis between Cd fractions, nutrient contents, and bacterial composition was further performed (Fig. S2). At phylum level, TN, SOM, TC, available K, and residual Cd content showed negative correlation with Acidobacteria, Elusimicobia, Latescibacteria, and Proteobacteria abundance, but positive to Actinobacteria and Cyanobacteria abundance (Fig. S2). At genus level, TN and available K content were positively correlated to *Devosia*, *Flavisolibacter*, *Massilia*, *Aeromicrobium*, *Iamia*, *Nocardioides*, *Pseudarthrobacter*, and *Marmoricola* abundance, but negatively to *Bacteroides*, *Haliangium*, and *MND1* abundance (Fig. S2). Unlike TN and available K, acid-soluble Cd content had significant negative correlation with *Devosia*, *Massilia*, *Aeromicrobium*, *Iamia*, *Nocardioides*, *Pseudarthrobacter*, and *Marmoricola* abundance, but was positively correlated to *Bacteroides*, *Haliangium*, and *MND1* abundance (Fig. S2). Spearman correlation result generally agreed to RDA result. Taken together, this study shed the advantages of DGB as soil amendment and guided to feasibly applying DGB to mitigate soil Cd-induced risk and acquiring underlying mechanisms.

5 Conclusions

Distiller's grain-derived biochar amendment promoted wheat growth in Cd-laden soil. Biochar rate and aging process jointly involved soil nutrient increase and Cd bioavailability decrease. Rising rate progressively increased soil pH and fertility but decreased soil Cd bioavailability by increasing residual Cd, thus more strongly promoting relative chlorophyll content and decreasing Cd uptake of wheat. As aging proceeded, although soil pH, organic matter, and total carbon contents somewhat dropped, residual Cd continuously increased to decrease Cd bioavailability via potential interactions of Cd with released Si and generated oxygenic groups of biochar during aging, which further decreased Cd uptake by most parts of wheat. Exceptionally, soil NO_3-N content progressively decreased with rising biochar rate and aging, partly due to the declined nitrifiers (e.g., Nitrosomonadaceae, Nitrospiraceae) abundance with rising biochar rate and aging. Rising biochar rate and aging jointly elevated the abundances of Actinobacteria, Cyanobacteria, and Fibrobacteria phyla and *Lysobacter*, *Massilia*, *Pseudarthrobacter*,

and *Iamia* genera that positively correlated to soil organic matter, residual Cd, total nitrogen, total carbon, and available K content. Thus, these key rhizospheric bacteria also contributed to soil fertility improvement and Cd fraction redistribution. Considering improved wheat growth/development and soil fertility and decreased Cd bioavailability and Cd uptake of wheat, amending 4% biochar with aging in soil was suitable scheme to promote soil fertility and minimize Cd-induced risk.

Supplementary Information The online version contains supplementary material available at https://doi.org/10.1007/s42729-023-01581-0.

Author Contribution **Chengyu Wang:** Formal analysis, investigation, writing — original draft. **Jieming Li:** Conceptualization; formal analysis; investigation; resources; writing, original draft; writing, review and editing; visualization; supervision; project administration; funding acquisition. **Lujun Chen:** Project administration, funding acquisition. **Xin Huang:** Project administration, funding acquisition.

Data Availability All data supporting the findings are available in this article and its supplementary information online.

Declarations

Ethics Approval All authors have read, understood, and complied with all requirements regarding the ethical responsibility of the journal.

Conflict of Interest The authors declare no competing interests.

References

Akca MO, Usta S, Uygur V, Ok SS (2023) Biochar applications reduces the mobility of cadmium under differing soil moisture regimes. Gesunde Pflanz 75:1047–1060. https://doi.org/10.1007/s10343-022-00753-9

Alvarenga P, Palma P, Goncalves AP, Baiao N, Fernandes RM, de Varennes A, Vallini G, Duarte E, Cunha-Queda AC (2008) Assessment of chemical, biochemical and ecotoxicological aspects in a mine soil amended with sludge of either urban or industrial origin. Chemosphere 72:1774–1781. https://doi.org/10.1016/j.chemosphere.2008.04.042

Alvarez A, Saez JM, Davila Costa JS, Colin VL, Fuentes MS, Cuozzo SA, Benimeli CS, Polti MA, Amoroso MJ (2017) Actinobacteria: current research and perspectives for bioremediation of pesticides and heavy metals. Chemosphere 166:41–62. https://doi.org/10.1016/j.chemosphere.2016.09.070

Bacosa HP, Inoue C (2015) Polycyclic aromatic hydrocarbons (PAHs) biodegradation potential and diversity of microbial consortia enriched from tsunami sediments in Miyagi, Japan. J Hazard Mater 283:689–697. https://doi.org/10.1016/j.jhazmat.2014.09.068

Bandara T, Franks A, Xu JM, Chathurika JBAJ, Tan CX (2021) Biochar aging alters the bioavailability of cadmium and microbial activity in acid contaminated soils. J Hazard Mater 420:126666. https://doi.org/10.1016/j.jhazmat.2021.126666

Basak BB, Maity A, Ray P, Biswas DR, Roy S (2022) Potassium supply in agriculture through biological potassium fertilizer: a promising and sustainable option for developing countries. Arch Agron Soil Sci 68:101–114. https://doi.org/10.1080/03650340.2020.1821191

Bashir S, Zhu J, Fu QL, Hu HQ (2018) Cadmium mobility, uptake and anti-oxidative response of water spinach (*Ipomoea aquatic*) under rice straw biochar, zeolite and rock phosphate as amendments. Chemosphere 194:579–587. https://doi.org/10.1016/j.chemosphere.2017.11.162

Beesley L, Moreno-Jimenez E, Gomez-Eyles JL, Harris E, Robinson B, Sizmur T (2011) A review of biochars' potential role in the remediation, revegetation and restoration of contaminated soils. Environ Pollut 159:3269–3282. https://doi.org/10.1016/j.envpol.2011.07.023

Chen DM, Chen DQ, Xue RR, Long J, Lin XH, Lin YB, Jia LH, Zeng RS, Song YY (2019) Effects of boron, silicon and their interactions on cadmium accumulation and toxicity in rice plants. J Hazard Mater 367:447–455. https://doi.org/10.1016/j.jhazmat.2018.12.111

Cheng YR, Bao YJ, Chen X, Yao Q, Wang C, Chai SY, Zeng J, Fan X, Kang HY, Sha LN, Zhang HQ, Zhou YH, Wang Y (2020) Different nitrogen forms differentially affect Cd uptake and accumulation in dwarf Polish wheat (*Triticum polonicum* L.) seedlings. J Hazard Mater 400:123209. https://doi.org/10.1016/j.jhazmat.2020.123209

Cheng JL, Li X, Xiao X, Yuan Y, Liao XP, Shi B, Zhang SY, Ao ZH (2021) Metal oxide loaded biochars derived from Chinese bai jiu distillers' grains used for the adsorption and controlled release of phosphate. Ind Crop Prod 173:114080. https://doi.org/10.1016/j.indcrop.2021.114080

Fan QY, Sun JX, Chu L, Cui LQ, Quan GX, Yan JL, Hussain Q, Iqbal M (2018) Effects of chemical oxidation on surface oxygen-containing functional groups and adsorption behavior of biochar. Chemosphere 207:33–40. https://doi.org/10.1016/j.chemosphere.2018.05.044

Gao X, Peng YT, Zhou YY, Adeel M, Chen Q (2019) Effects of magnesium ferrite biochar on the cadmium passivation in acidic soil and bioavailability for packoi (*Brassica chinensis* L.). J Environ Manage 251:109610. https://doi.org/10.1016/j.jenvman.2019.109610

Gao RL, Xiang L, Hu HQ, Fu QL, Zhu J, Liu YH, Huang GY (2020) High-efficiency removal capacities and quantitative sorption mechanisms of Pb by oxidized rape straw biochars. Sci Total Environ 699:134262. https://doi.org/10.1016/j.scitotenv.2019.134262

Gillan DC, Danis B, Pernet P, Joly G, Dubois P (2005) Structure of sediment-associated microbial communities along a heavy-metal contamination gradient in the marine environment. Appl Environ Microbiol 71:679–690. https://doi.org/10.1128/AEM.71.2.679-690.2005

Hamid Y, Tang L, Hussain B, Usman M, Hashmi MLUR, Khan MB, Yang XE, He ZL (2020) Immobilization and sorption of Cd and Pb in contaminated stagnic anthrosols as amended with biochar and manure combined with inorganic additives. J Environ Manage 257:109999. https://doi.org/10.1016/j.jenvman.2019.109999

Houben D, Sonnet P (2015) Impact of biochar and root-induced changes on metal dynamics in the rhizosphere of *Agrostis capillaris* and *Lupinus albus*. Chemosphere 139:644–651. https://doi.org/10.1016/j.chemosphere.2014.12.036

Huang DL, Liu LS, Zeng GM, Xu P, Huang C, Deng LJ, Wang RZ, Wan J (2017) The effects of rice straw biochar on indigenous microbial community and enzymes activity in heavy metal-contaminated sediment. Chemosphere 174:545–553. https://doi.org/10.1016/j.chemosphere.2017.01.130

Jabbrova D, Abdrakhmanov T, Jabbrova Z, Abdullaev S, Azimov A, Mohamed I, AlHarbi M, Abu-Elsaoud A, Elkelish A (2023) Biochar improves the growth and physiological traits of alfalfa, amaranth and maize grown under salt stress. PeerJ 11:e15684. https://doi.org/10.7717/peerj.15684

Khan I, Awan SA, Rizwan M, Ali S, Hassan MJ, Brestic M, Zhang XQ, Huang LK (2021) Effects of silicon on heavy metal uptake at soil-plant interphase: a review. Ecotoxicol Environ Safe 222:112510. https://doi.org/10.1016/j.ecoenv.2021.112510

Kuppusamy S, Thavamani P, Megharaj M, Venkateswarlu K, Lee YB, Naidu R (2016) Pyrosequencing analysis of bacterial diversity in soils contaminated long-term with PAHs and heavy metals: implications to bioremediation. J Hazard Mater 317:169–179. https://doi.org/10.1016/j.jhazmat.2016.05.066

Li D, Hockaday WC, Masiello CA, Alvarez PJJ (2011) Earthworm avoidance of biochar can be mitigated by wetting. Soil Biol Biochem 43:1732–1737. https://doi.org/10.1016/j.soilbio.2011.04.019

Li JM, Cao LR, Yuan Y, Wang RP, Wen YZ, Man JY (2018) Comparative study for microcystin-LR sorption onto biochars produced from various plant- and animal-wastes at different pyrolysis temperatures: influencing mechanisms of biochar properties. Bioresour Technol 247:794–803. https://doi.org/10.1016/j.biortech.2017.09.120

Lian GQ, Wang B, Lee XQ, Li L, Liu TZ, Lyu WQ (2019) Enhanced removal of hexavalent chromium by engineered biochar composite fabricated from phosphogypsum and distillers grains. Sci Total Environ 697:134119. https://doi.org/10.1016/j.scitotenv.2019.134119

Liu YZ, Liu SP, Huang CH, Ge XY, Xi BD, Mao J (2022) Chinese Baijiu distiller's grains resourcing: current progress and future prospects. Resour Conserv Recy 176:105900. https://doi.org/10.1016/j.resconrec.2021.105900

Luo WC, Qian L, Liu WW, Zhang X, Wang Q, Jiang HY, Cheng BJ, Ma H, Wu ZY (2021) A potential Mg-enriched biochar fertilizer: excellent slow-release performance and release mechanism of nutrients. Sci Total Environ 768:144454. https://doi.org/10.1016/j.scitotenv.2020.144454

Martin SM, Kookana RS, Van Zwieten L, Krull E (2012) Marked changes in herbicide sorption-desorption upon ageing of biochars in soil. J Hazard Mater 231:70–78. https://doi.org/10.1016/j.jhazmat.2012.06.040

Meng ZW, Huang S, Laird DA, Wu JW, Lin ZB (2022) Identifying key processes driving Cd long-term adsorption and immobilization by biochar in soils and evaluating combined aging effects under simulated local climates. J Environ Chem Eng 10:108636. https://doi.org/10.1016/j.jece.2022.108636

Mukherjee A, Zimmerman AR, Harris W (2011) Surface chemistry variations among a series of laboratory-produced biochars. Geoderma 163:247–255. https://doi.org/10.1016/j.geoderma.2011.04.021

Mukherjee A, Zimmerman AR, Hamdan R, Cooper WT (2014) Physicochemical changes in pyrogenic organic matter (biochar) after 15 months of field aging. Solid Earth 5:693–704. https://doi.org/10.5194/se-5-693-2014

Nie TH, Yang X, Chen HB, Muller K, Shaheen SM, Rinklebe J, Song H, Xu S, Wu FC, Wang HL (2021) Effect of biochar aging and co-existence of diethyl phthalate on the mono-sorption of cadmium and zinc to biochar-treated soils. J Hazard Mater 408:124850. https://doi.org/10.1016/j.jhazmat.2020.124850

Norton JM, Stark JM (2011) Regulation and measurement of nitrification in terrestrial systems. Methods Enzymol 486:343–368. https://doi.org/10.1016/S0076-6879(11)86015-5

Puopolo G, Tomada S, Pertot I (2018) The impact of the omics era on the knowledge and use of Lysobacter species to control phytopathogenic micro-organisms. J Appl Microbiol 124:15–27. https://doi.org/10.1111/jam.13607

Qian LB, Chen BL (2014) Interactions of aluminum with biochars and oxidized biochars: implications for the biochar aging process. J Agr Food Chem 62:373–380. https://doi.org/10.1021/jf404624h

Rehman MZ, Rizwan M, Ali S, Fatima N, Yousaf B, Naeem A, Sabir M, Ahmad HR, Ok YS (2016) Contrasting effects of biochar, compost and farm manure on alleviation of nickel toxicity in maize (Zea mays L.) in relation to plant growth, photosynthesis and metal uptake. Ecotoxicol Environ Safe 133:218–225. https://doi.org/10.1016/j.ecoenv.2016.07.023

Seccareccia I, Kost C, Nett M (2015) Quantitative analysis of Lysobacter predation. Appl Environ Microbiol 81:7098–7105. https://doi.org/10.1128/AEM.01781-15

Shaheen SM, Niazi NK, Hassan NEE, Bibi I, Wang H, Tsang DCW, Ok YS, Bolan N, Rinklebe J (2018) Wood-based biochar for the removal of potentially toxic elements in water and wastewater: a critical review. Int Mater Rev 64:216–247. https://doi.org/10.1080/09506608.2018.1473096

Shi RY, Li JY, Ni N, Xu RK (2019) Understanding the biochar's role in ameliorating soil acidity. J Integr Agr 18:1508–1517. https://doi.org/10.1016/S2095-3119(18)62148-3

Spokas KA (2010) Review of the stability of biochar in soils: predictability of O: C molar ratios. Carbon Manage 1:289–303. https://doi.org/10.4155/CMT.10.32

Tan LS, Ma ZH, Yang KQ, Cui QL, Wang K, Wang TT, Wu GL, Zheng JY (2020) Effect of three artificial aging techniques on physicochemical properties and Pb adsorption capacities of different biochars. Sci Total Environ 699:134223. https://doi.org/10.1016/j.scitotenv.2019.134223

Usman M, Zia-ur-Rehman M, Rizwan M, Abbas T, Ayub MA, Naeem A, Alharby HF, Alabdallah NM, Alharbi BM, Qamar MJ, Ali S (2023) Effect of soil texture and zinc oxide nanoparticles on growth and accumulation of cadmium by wheat: a life cycle study. Environ Res 216(Part 1):114397. https://doi.org/10.1016/j.envres.2022.114397

Wang MM, Zhu Y, Cheng LR, Anderson B, Zhao XH, Wang DY, Ding AZ (2018) Review on utilization of biochar for metal-contaminated soil and sediment remediation. J Environ Sci 63:156–173. https://doi.org/10.1016/j.jes.2017.08.004

Wang L, Wang LA, Zhan XY, Huang YK, Wang J, Wang X (2020) Response mechanism of microbial community to the environmental stress caused by the different mercury concentration in soils. Ecotoxicol Environ Safe 188:109906. https://doi.org/10.1016/j.ecoenv.2019.109906

Wang YF, Zhang K, Lu L, Xiao X, Chen BL (2020) Novel insights into effects of silicon-rich biochar (Sichar) amendment on cadmium uptake, translocation and accumulation in rice plants. Environ Pollut 265:114772. https://doi.org/10.1016/j.envpol.2020.114772

Wang YL, Xu YM, Liang XF, Wang L, Sun YB, Huang QQ, Qin X, Zhao LJ (2021) Soil application of manganese sulfate could reduce wheat Cd accumulation in Cd contaminated soil by the modulation of the key tissues and ionomic of wheat. Sci Total Environ 770:145328. https://doi.org/10.1016/j.scitotenv.2021.145328

Xu XY, Kan Y, Zhao L, Cao XD (2016) Chemical transformation of CO$_2$ during its capture by waste biomass derived biochars. Environ Pollut 213:533–540. https://doi.org/10.1016/j.envpol.2016.03.013

Xu CB, Zhao JW, Yang WJ, He L, Wei WX, Tan X, Wang J, Lin AJ (2020) Evaluation of biochar pyrolyzed from kitchen waste, corn straw, and peanut hulls on immobilization of Pb and Cd in contaminated soil. Environ Pollut 261:114133. https://doi.org/10.1016/j.envpol.2020.114133

Yang WT, Zhou H, Gu JF, Liao BH, Zhang J, Wu P (2020) Application of rapeseed residue increases soil organic matter, microbial biomass, and enzyme activity and mitigates cadmium pollution risk in paddy fields. Environ Pollut 264:114681. https://doi.org/10.1016/j.envpol.2020.114681

Yao FX, Arbestain MC, Virgel S, Blanco F, Arostegui J, Macia-Agullo JA, Macias F (2010) Simulated geochemical weathering of a

mineral ash-rich biochar in a modified Soxhlet reactor. Chemosphere 80:724–732. https://doi.org/10.1016/j.chemosphere.2010.05.026

Yao RJ, Li HQ, Yang JS, Wang XP, Xie WP, Zhang X (2022) Biochar addition inhibits nitrification by shifting community structure of ammonia-oxidizing microorganisms in salt-affected irrigation-silting soil. Microorganisms 10:436. https://doi.org/10.3390/microorganisms10020436

Yu XX, Zhao JT, Liu XQ, Sun LX, Tian J, Wu NF (2021) Cadmium pollution impact on the bacterial community structure of arable soil and the isolation of the cadmium resistant bacteria. Front Microbiol 12:698834. https://doi.org/10.3389/fmicb.2021.698834

Yuan XH, Xue ND, Han ZG (2021) A meta-analysis of heavy metals pollution in farmland and urban soils in China over the past 20 years. J Environ Sci 101:217–226. https://doi.org/10.1016/j.jes.2020.08.01.3

Yuan Y, Li JM, Dai HX (2021) Microcystin-LR sorption and desorption by diverse biochars: capabilities, and elucidating mechanisms from novel insights of sorption domains and site energy distribution. Sci Total Environ 754:141921. https://doi.org/10.1016/j.scitotenv.2020.141921

Yuan Y, Li JM, Wang CY, An GQ (2021) Contrasting microcystin-LR sorption and desorption capability of different farmland soils amended with biochar: effects of biochar dose and aging time. Environ Pollut 286:117364. https://doi.org/10.1016/j.envpol.2021.117364

Yuan CP, Gao BL, Peng YT, Gao X, Fan BB, Chen Q (2021) A meta-analysis of heavy metal bioavailability response to biochar aging: importance of soil and biochar properties. Sci Total Environ 756:144058. https://doi.org/10.1016/j.scitotenv.2020.144058

Zhang XK, Wang HL, He LZ, Lu KP, Sarmah A, Li JW, Bolan N, Pei JC, Huang HG (2013) Using biochar for remediation of soils contaminated with heavy metals and organic pollutants. Environ Sci Pollut Res 20:8472–8483. https://doi.org/10.1007/s11356-013-1659-0

Zhang XK, Sarmah AK, Bolan NS, He LZ, Lin XM, Che L, Tang CX, Wang HL (2016) Effect of aging process on adsorption of diethyl phthalate in soils amended with bamboo biochar. Chemosphere 142:28–34. https://doi.org/10.1016/j.chemosphere.2015.05.037

Zhang YF, Wang JM, Feng Y (2021) The effects of biochar addition on soil physicochemical properties: a review. CATENA 202:105284. https://doi.org/10.1016/j.catena.2021.105284

Zhao Y, Li JM (2022) Effect of varying pH and co-existing microcystin-LR on time- and concentration-dependent cadmium sorption by goethite-modified biochar derived from distillers' grains. Environ Pollut 307:119490. https://doi.org/10.1016/j.envpol.2022.119490

Zheng BX, Bi QF, Hao XL, Zhou GW, Yang XR (2017) *Massilia phosphatilytica* sp. nov., a phosphate solubilizing bacteria isolated from a long-term fertilized soil. Int J Syst Evol Microbiol 67:2514–2519. https://doi.org/10.1099/ijsem.0.001916

Zhou J, Zhang C, Du BY, Cui HB, Fan XJ, Zhou DM, Zhou J (2020) Effects of zinc application on cadmium (Cd) accumulation and plant growth through modulation of the antioxidant system and translocation of Cd in low- and high-Cd wheat cultivars. Environ Pollut 265:115045. https://doi.org/10.1016/j.envpol.2020.115045

Zuo YY, Li Y, Chen H, Ran G, Liu XM (2023) Effects of multi-heavy metal composite pollution on microorganisms around a lead-zinc mine in typical karst areas, southwest China. Ecotoxicol Environ Safe 262:115190. https://doi.org/10.1016/j.ecoenv.2023.115190